

## **Latest prospects in coastal pollution monitoring via remote sensing of ocean colour**

**Sandrine Mathieu <sup>1</sup>, Claire-Anne Reix <sup>1</sup>, Audrey Minghelli-Roman <sup>2</sup>,  
Laurent Polidori <sup>3</sup>, Lionel Loubersac <sup>4</sup> and François Cauneau <sup>5</sup>**

<sup>1</sup> Alcatel Alenia Space, Cannes-la-Bocca, France

<sup>2</sup> Université de Bourgogne LE2I, UMR-CNRS 5158 21078, Dijon, France

<sup>3</sup> IRD Laboratoire Régional de Télédétection, Cayenne, Guyane, France

<sup>4</sup> IFREMER DEL-DRV LER/LR, Sète, France

<sup>5</sup> Ecole des Mines de Paris, Centre d'Energique, Sophia-Antipolis, France

### **ABSTRACT**

Remote detection enables the acquisition of large volumes of data in particular in areas which are not accessible. This paper describes shortly the main use of remote sensing for oceanography and marine applications. Then it presents a study related to lagoon pollution based on the Medium Resolution Imaging Spectrometer (MeRIS) which was launched in March 2002 and has been providing images since June 2002. Before its launch, we had implemented a method to improve its resolution by merging its images with Landsat Enhanced Thematic Mapper images in order to preserve the best characteristics of the two images (spatial, spectral, temporal). We now present the results of this method for real MeRIS images (level 1b and 2) in a coastal area. The robustness of the method is studied as well as the influence of the delay between the acquisition of the two images.

### **1. INTRODUCTION**

Remote detection enables the acquisition of large volumes of data on the world's oceans and coastal regions, allowing scientists to observe events in remote and often inaccessible regions. These data can then be used for a variety of applications, such as mapping ocean dynamics and monitoring coastal change. These two functions-ocean modeling and coastal monitoring are either deployed directly or integrated in order to forecast changes in the phenomena detected and to optimize action plans. Such phenomena include oil slick drift, assessing changes in coastal pollution and the proliferation of algae.

One particular aspect of ocean and coastal phenomena modeling is the monitoring of lagoon pollution episodes. Alcatel Alenia Space, IFREMER (Institut Français de Recherche pour l'Exploitation de la Mer, IRD (Institut de Recherche pour le Développement), the University of Bourgogne and Ecole des Mines have teamed up to demonstrate the potential capabilities of satellite imaging applications in this area. This type of pollution has a direct impact on shellfish farming and thus on human health. Modeling phenomena over long periods, forecasting pollution episodes, rapidly detecting known pollution and tracking its change are priority objectives for the

agencies responsible for managing coastal zones. We worked closely with these satellite data users to conduct the study presented in this document.

### **Ocean forecasting**

Oceanography uses data collected via remote detection to determine the direction and strength of currents, the amplitude and direction of surface winds and to measure sea surface temperature. Operational monitoring and forecasting, which is the focus of the integrated European marine environment and security program, MERSEA (coordinated by IFREMER), leverages the significant advances made in satellite altimetry, notably the TOPEX/POSEIDON and Jason altimeter radars which measure wave height and enable high-precision observation from space of changes in sea levels. These data are integrated with *in situ* surface and depth measurements into models that constitute regional and global “snapshots” of ocean change. Operational oceanography, which provides data on all aspects of the Earth’s oceans, also uses other types of space data: scatterometers, which measure wind speed and direction, synthetic aperture radars, which measure changes in sea surface roughness due to winds and currents, as well as active radiometers and microwave sensors, which provide ocean surface temperature data.

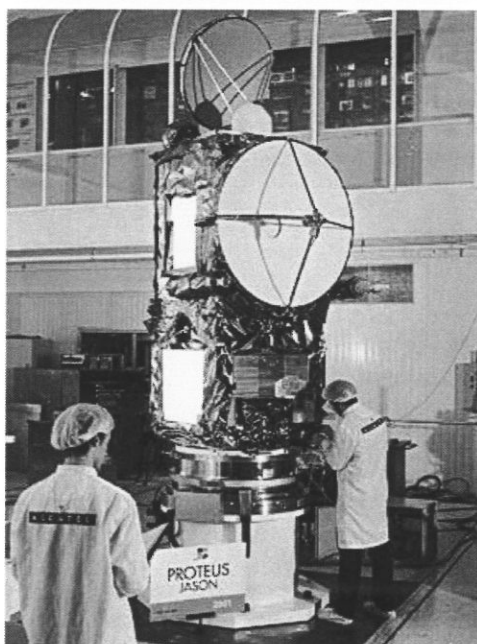


Fig. 1. Jason in Alcatel Alenia Space clean rooms.

### **Ocean and coastal surveillance**

Remote detection applications for ocean and coastal surveillance activities include: pollution detection (oil slicks, watershed discharge, water quality monitoring—with regard to farming, bathing, protected zones, etc.), assessment of phytoplankton concentration and algae proliferation, inventory and monitoring of aquaculture, evaluation of resources, definition of fishing quotas and monitoring of fishing practices, maritime traffic tracking (density, protected zones, etc.), coastal cartography (changes in coast lines, beach dynamics), protection of coastal regions, and the impact of anthropogenic activities.

Spatial optics and radar are the major components in ocean and coastal surveillance. Very high-resolution (superspectral and hyperspectral) data is required to measure the color of oceans. Furthermore, extensive spatial coverage provides a synoptic view of the distribution and spatial variability of chlorophyll (phytoplankton), water temperature, and concentration of suspended matter. Hyperspectral data provided by such instruments as MeRIS or MODIS (gathered in

several narrow and near-infrared bands of the visible spectrum) allow enhanced precision in the classification of objects under study. For example, hyperspectral data are used today to obtain the cartography of regional time and spatial models of ocean color. The color of the ocean is determined by water quality, with chlorophyll one of the main indicators. Monthly and seasonal images are required for comprehensive modeling.

Hyperspectral data also provides information on water turbidity, bottom bathymetry and cartography in coastal zones.

Radar data provide additional information during nighttime observation or cloudy weather when optical data is not available. Radar data are also used in a wide range of applications, especially for detecting marine pollution. Oil slicks, for example, inhibit ocean waves, creating a surface which is smoother than the surrounding water. A weaker signal is returned to the imaging radar, producing a black line on the image. The direction of the slick and its predicted drift are determined using the operational oceanographic data described above, along with the meteorological data integrated into drift models in order to optimize rescue and clean-up operations. In addition, high-resolution radar imaging instruments enable the detection of polluting ships (identified as a lighter spot on the image).

Images captured by satellite sensors harbor huge potential for a rich variety of applications. Among them, pollution monitoring is of particular interest. Users of satellite images already benefit from a broad array of regular and long-term services. From a global perspective, the combination of satellite data and information gathered by airborne or ship-borne *in situ* sensors and integrated into models today makes it possible to provide a pertinent response to ocean management.

At the same time, further progress can be achieved. The burgeoning array of technical advances in spatial sensors, coupled with their improved revisit rate, should enable the development of additional applications to provide even more sophisticated services.

## 2. OCEAN COLOUR MONITORING

OCEAN colour monitoring is usually based on optical remote sensing with spatial resolutions around 1 km. This spatial scale is available with such sensors as NOAA's Advanced Very High Resolution Radiometer, the Polarization and Directionality of the Earth's Reflectances Instrument, or Sea-viewing Wide Field-of-view Sensor, which cover one to several thousand kilometers in a single swath and provide very short revisit periods. The Medium Resolution Imaging Spectrometer (MeRIS) sensor, launched on board ENVISAT in 2002, was designed for sea colour observation, with a 300-meter spatial resolution, 15 programmable spectral bands and a three day revisit period. Three hundred meter is a high resolution for an oceanographic sensors but it is still too rough for coastal water monitoring, where physical and biological phenomena require better spatial resolution (Minghelli, 1999). On the opposite, multispectral Landsat Enhanced Thematic Mapper (ETM) images offer a suitable spatial resolution, but have only four spectral bands in the visible and near infrared spectrum, allowing poor spectral characterization. A few years ago, in order to combine the spectral resolution of MeRIS and the spatial resolution of Landsat ETM, we implemented a merging method proposed by Zhukov *et al.* (1999). Before the launch of ENVISAT, we applied this method to simulated MeRIS images (Minghelli-Roman *et al.*, 2001).

This method is now applied to real MeRIS images. Two product levels are considered. Level 1b contains radiance measurements at the top of the atmosphere for the calibrated and geocoded fifteen (15) MeRIS bands. Level 2 contains normalized surface reflectance and several geophysical and biophysical parameters such as algal pigment index, suspended sediment, Rayleigh-corrected Vegetation Indices, aerosol type, cloud albedo. The method was tested for radiance (level 1b) and reflectance (level 2) over a coastal area of approximately 30x30 km<sup>2</sup> located around the Thau lagoon (southern France).

The main steps of the method are briefly recalled and the results are presented for levels 1b and 2. A validation method is proposed based on a statistical quality criterion, namely, the ERGAS parameter. In a previous paper we had suggested that the delay between the two images could

have an impact on the fusion relevance in case of landscape evolution. This constraint is analysed as well. Eventually, the potential and limitations of this resolution improvement approach are discussed.

### 3. MeRIS – ETM MERGING METHOD

ETM images have high spatial resolution and low spectral resolution compared to MeRIS images. A MeRIS-ETM merging method was presented in detail by Minghelli-Roman *et al.* (2001). First, the MeRIS image is geometrically co-registered with the ETM image. Then, a multispectral classification is applied to the ETM image in order to divide its pixels into  $N_C$  classes. The only request is that all pixels must belong to a class (i.e. no pixel remains unclassified).

Each MeRIS pixel covers 100 pixels of the ETM classification. The proportion of each class is computed within each MeRIS pixel. For each class, a mean spectral profile is obtained by solving an algebraic system. The last step consists of substituting each classified pixel with its corresponding spectral profile. The output image is a 30 m spatial resolution (ETM spatial resolution) and 15 spectral bands (MeRIS spectral resolution).

For MeRIS level 2 images, we noticed that “black pixels” were located on land-water borders. Since atmospheric corrections use different methods on land and water, these mixed pixels are not corrected and their MeRIS level 2 reflectance is set to zero for all spectral bands. These pixels are used neither to solve the algebraic system nor to determine the spectral profile of the class. In order not to leave black pixels in the resulting image, we replace the classified ETM pixels by the spectral profile obtained for the pixels belonging to the same class.

For all images, the number of classes has been optimised. Classifications have been run on the ETM image with different numbers of classes in order to assess the influence of this number on the fusion output.

The ERGAS parameter, based on an RMSE estimation (Ranchin *et al.*, 2003), is chosen as a robustness criterion (1). This statistical parameter is often used for evaluation of fusion techniques (Wehrmann *et al.*, 2005). It compares the absolute radiometric values between MeRIS original image and the one resulting from the fusion. Resolution of pixels resulting from the fusion is degraded to 300 m to be compared to the original MeRIS ones. This subsampling was performed by pixel averaging, thus considering the MeRIS Modulation Transfer Function (MTF) as perfect for the resolution decrease. This approximation has statistically no effect on the comparison.

$$\text{ERGAS}(X, Y) = 100 * \frac{h}{l} \sqrt{\frac{1}{nb} \sum_{\lambda=1}^{nb} \frac{[\text{RMSE}(X, Y, \lambda)]^2}{[\text{mean}(X - Y, \lambda)]^2}} \quad (1)$$

with

X original MeRIS image,  
Y resulting image of fusion,  
h the ETM resolution (30m),  
l the MeRIS resolution (300m),  
 $\lambda$  the spectral band,  
nb the total number of spectral bands.

The ERGAS is affected by two main factors. The first is the classification applied to the ETM image. It reduces the radiometric variability. The number of classes has no intrinsic physical significance. It is only a consequence of the radiometric variability within the TM image.

The second factor is the delay between the two image acquisitions. It increases the probability of landscape changes. If the classification applied to ETM is merged with a MeRIS image acquired a long time later, the fusion may become inconsistent.

## 4. RESULTS

### A. Results on MeRIS level 1b images (see Figure 3)

Figure 2 shows that the optimal number of classes is around 100 with an ERGAS parameter equal to 1.00. Figure 3a shows a colour composite of the input ETM image (1000x1000 pixels) and Figure 3b the input MeRIS image (100x100 pixels) in radiance. A zoom factor of 10 has been applied to this image in order to emphasise the difference between ETM and MeRIS resolutions. Eventually, the resulting fusion image (Figure 3c) is characterized by 15 spectral bands and a 30 m resolution. A spatial improvement is visible when comparing Figure 3b,c.

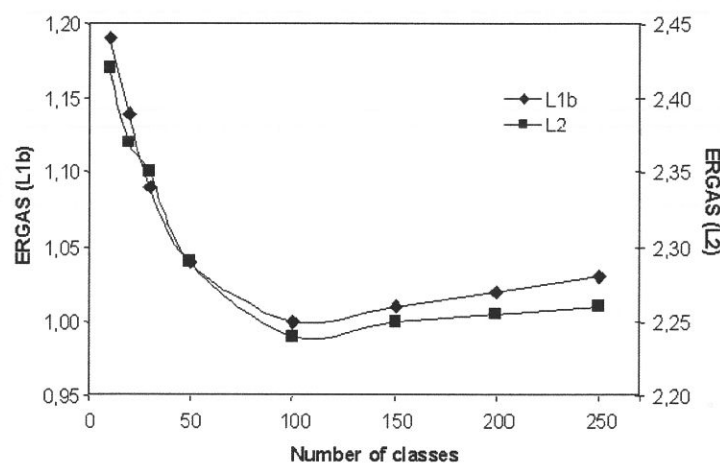


Fig. 2. ERGAS versus number of classes. The optimal number of classes is given by the minimum value of the ERGAS parameter, i.e. 100 for level 1b and 2 images.

MeRIS image spectra are well preserved, as suggested by the colour image, as well as the geometric resolution of the ETM image. The output image has the spatial characteristics of ETM and the spectral and radiometric characteristics of MeRIS (radiance image).

### B. Results on MeRIS Level 2 images

The same fusion has been applied to the same MeRIS image but on the level 2 product. The optimal number of classes is also 100, and the ERGAS parameter is then equal to 2.24. This difference in ERGAS parameter values is mainly due to the artefact that MeRIS level 2 images exhibit some "black pixels" located on land-water borders.

Comparing the number of classes with the simulated case (equal to 150 (Minghelli-Roman *et al.*, 2001)), we remark that different radiometric and geomorphologic conditions provide different optimizations.

## 5. TEMPORAL CONSTRAINS DUE TO LANDSCAPE EVOLUTION

The revisit period of an imaging sensor depends on satellite orbit and on viewing geometry (off-nadir angle and swath width). The revisit periods of MeRIS and ETM being different and not synchronized, fusion can generally not be applied to images acquired simultaneously. Because ETM Landsat has a long revisit period (image acquisitions can occur every 16 days at minimum, and much more in cloudy conditions) and MeRIS has a wide swath (images can be acquired more frequently i.e. every three days at minimum), the fusion of ETM and MeRIS can then become inconsistent if the landscape has changed between the two acquisitions.

For example, heliosynchronous orbits are not synchronized with tide cycles, so that two images have no reason for having the same tide elevation. This may be a severe limitation in coastal areas. Similarly, seasonal landscape changes appear if the time delay exceeds a few months. The

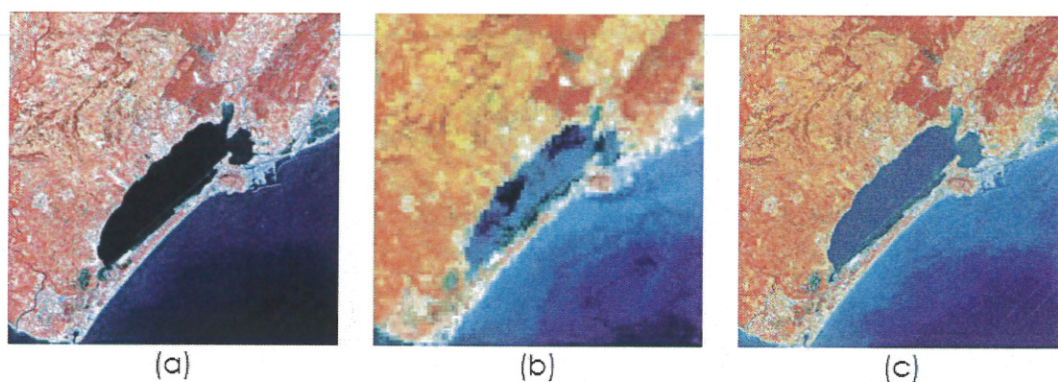


Fig. 3. (a) ETM Colour Composite (30m, 6 spectral bands); (b) MeRIS (Level 1b) Colour Composite (300m, 15 spectral bands) acquired on August 14, 2002; (c) fusion result (30m, 15 spectral bands).

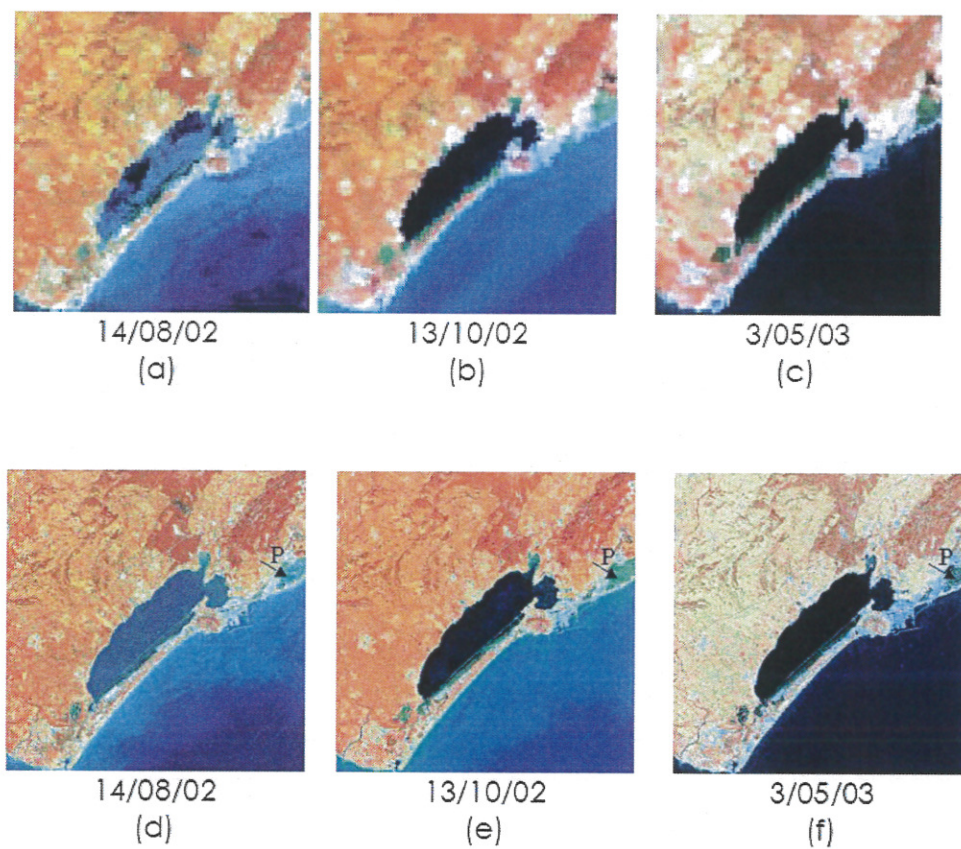


Fig. 4. MeRIS (Level 1b) colour composite images. (a) 14 August, 2002; (b) 13 October, 2002; (c) 3 May, 2003; (d), (e), (f) fusion results (ETM and MeRIS level 1b) for the same dates.

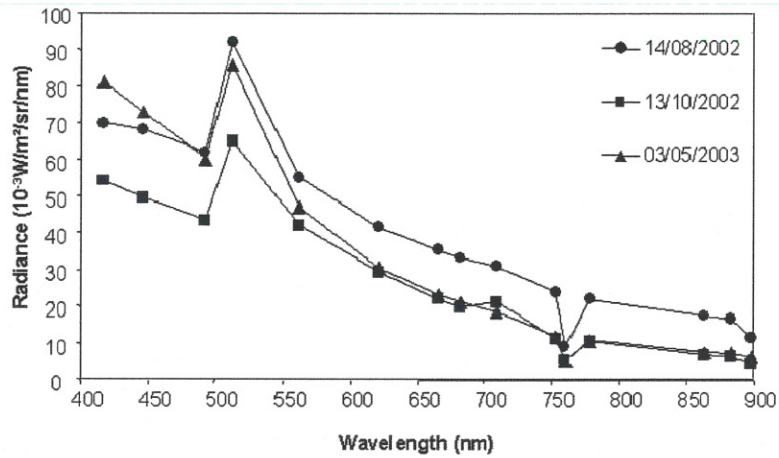


Fig. 5. Temporal spectral profile of the pixel indicated as P in Figure 4 (in radiance).

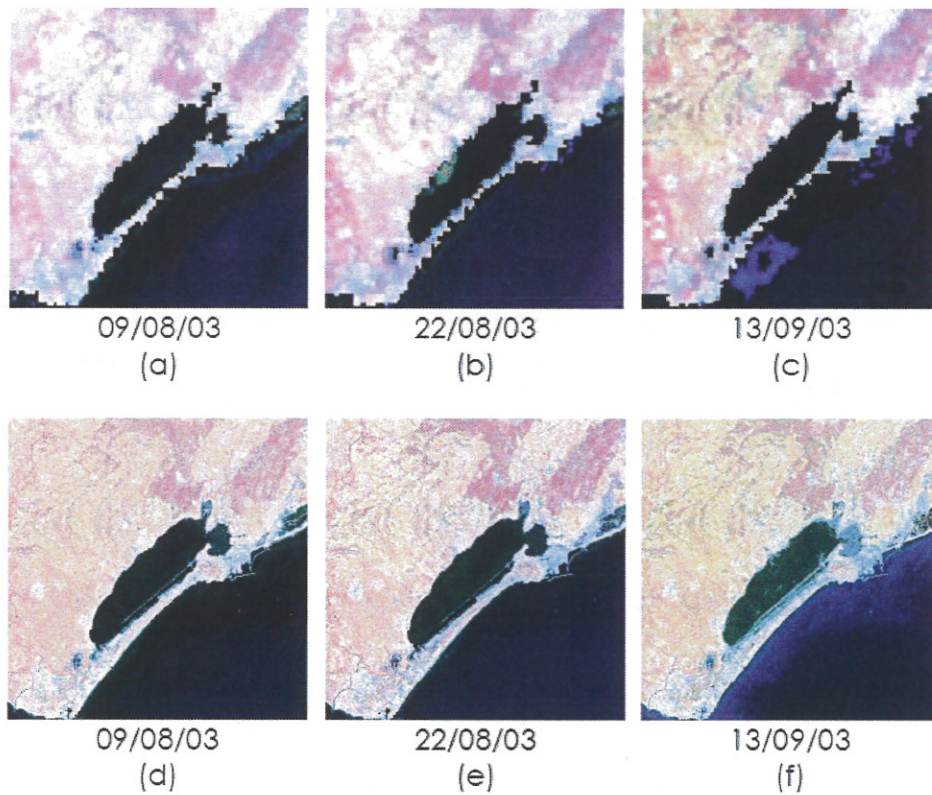


Fig. 6. MeRIS (Level 2) colour composite images. (a) 9 September, 2003; (b) 22 August, 2003; (c) 13 September, 2003; (d), (e), (f) fusion results (ETM and MeRIS level 2) for the same dates.

robustness of the fusion may then be evaluated with the increasing delay between ETM and MeRIS images acquisition.

#### *A. Results on MeRIS level 1b images (see Figure 4)*

The same ETM image (1000\*1000 pixels) acquired on 16 August, 2002 has been merged with three different MeRIS level 1b images acquired on 14 August, 2002, 13 October, 2002 and 3 May, 2003. The delays between ETM and MeRIS images are respectively two days, two months and nine months. All MeRIS images have been geometrically co-registered with the ETM image. Figure 4a,b,c shows these three MeRIS images (100\*100 pixels).

A radiometric evolution can be observed between MeRIS images due to seasonal changes. The first image has been acquired in summer, the second one in autumn and the last in the spring. We note that inland pixels have brighter tones in the second image than in the third, because of the higher photosynthesis activity in spring.

The assumption of the geometric stability between the two acquisitions has been made. If necessary this assumption will be verified during the validation, by using the ERGAS parameter. Figure 4d,e,f shows the visual results of these fusions.

A visual comparison shows that the seasonal landscape evolutions are preserved. With the fusion, the spectral evolution of a landscape object can be tracked in the ETM image. Figure 5 shows the spectral evolution of the pixel indicated as point P, located at the middle of a pond, to the east of Thau lagoon.

Figure 5 shows a decrease of the chlorophyll peak between 14 August, 2002 and 13 October, 2002 and an increase between 13 October, 2002 and May 3, 2003. This evolution is explained by a strong eutrophication of some lagoons which receive fluvial waters containing organic matter and chemical fertilizers from cultivated fields situated upstream in watersheds. This eutrophication increases in summer under specific atmospheric conditions, decreases in autumn and winter and increases again in spring.

#### *B. Results on MeRIS level 2 images (see Figure 6)*

The same ETM image (1000\*1000 pixels) acquired on 16 August, 2002 has been merged with three different MeRIS Level 2 images acquired on 9 September, 2003, 22 August, 2003 and 13 September, 2003. The image acquisition dates are different from level 1 images. The objective is not to compare the results between level 1 and level 2 images (the results would have been similar) but to show that the fusion is possible between two image levels according to the required product. The delays between ETM and MeRIS image acquisitions are respectively 358, 371 days and 393 days. MeRIS images have been geometrically co-registered on the ETM image. Figure 6a,b,c shows these three extracts of MeRIS images (100\*100 pixels).

The pale colours of MeRIS images are due to atmospheric corrections which use different methods on land and water. The black pixel artefact for level 1b images is noticed on land-water borders (Figure 6a,b,c). The image of the 13 September, 2003 has many pale blue pixels which are the result of inaccurate land-water masking.

The 22 August, 2003 image shows a bright spot on the Thau lagoon, produced by an anoxic crisis. This crisis was due to the eutrophication and was resulting from specific meteorological and environmental conditions.

Figure 6d,e,f shows the fusion results for the three dates. One can notice that MeRIS radiometric values are globally preserved on water and land. Black pixels have also disappeared and have been replaced by reflectance values computed from other pixels of the same class located somewhere else in the image as explained in the method description. It is particularly noticeable on Figure 6f where the fusion has removed a important black pixel artefact.

A typical temporal effect can be seen in Figure 6e, where the lighter spot on the Thau lagoon disappeared. It is due to its absence in the original ETM image. The high reflectance of this spot has then been "diluted" in the other classes covering the Thau lagoon. This phenomenon confirms that this fusion method is only valid for a landscape with limited changes between the



acquisition dates of ETM and MeRIS. Indeed, the spectral profile of a landscape object can be monitored only if it is present in the original ETM image.

Results of the ERGAS parameter calculation are given in Table 1 and Table 2.

Table 1 shows that the ERGAS parameter increases with the delay between images acquisitions. This confirms the temporal limitation of our fusion method. Ranchin *et al.* (2003) have empirically fixed a fusion validity limit for ERGAS = 3. The first three fusions with MeRIS level 1b images are valid because the landscape has not geometrically changed between the two dates.

Table 1. MeRIS Level 1: date acquisition, delay, between ETM and MeRIS acquisition, ERGAS parameter.

Image	Date	Delay between ETM and MeRIS acquisitions (days)	ERGAS
TM	16/08/02		
MeRIS level 1	14/08/02	-2	1.05
	13/10/02	58	1.33
	03/05/03	260	1.92

The fusion with MeRIS level 2 images is more critical as revealed by the ERGAS parameter which exceeds or is close to 3. Two reasons explain these high values, first the important delay between the two images acquisitions minimum 358 days, second the apparition of the lighter spot on the Thau lagoon which brought a geometrical change into the landscape. However, the ERGAS values given in Table 1 and 2 cannot be compared by absolute values because level 2 images are not obtained by a linear transformation from level 1b images.

Table 2. MeRIS Level 2: date acquisition, delay, between ETM and MeRIS acquisition, ERGAS parameter.

Image	Date	Delay between ETM and MeRIS acquisitions (days)	ERGAS
TM	16/08/02		
MeRIS level 2	09/08/03	358	3.88
	22/08/03	371	2.86
	13/09/03	393	4.66

## 6. DISCUSSION

The method proposed for MeRIS spatial resolution improvement has several advantages. Classical unmixing methods (Hu *et al.*, 1999; Settel and Drake, 1993) require an *a priori* knowledge of end-members and their spectral profiles. This knowledge requires minimum ground information and becomes meaningless if the image does not contain pure pixels. For such methods, the number of end-members cannot exceed the number of spectral bands in order to make the system invertible and therefore to ensure that one solution exists. For the chosen fusion method, the number of end-members is only bounded by the number of available pixels in the low resolution image.

While classical methods handling absolute spectra require absolute calibration and atmospheric, directional and topographic corrections in the radiometric preprocessing, these are not required for this method.

Beyond these operational advantages, the most interesting potential of this method is the effective resolution improvement due to the fusion with a higher resolution image, while other methods only provide a proportion of each end-member inside each pixel without any subpixel location information.

However, some limitations need to be considered, some of which have already been identified (Minghelli-Roman *et al.*, 2001). For example, first the merged image is only an approximation of the pseudo image acquired by a virtual 30 m resolution and 15 spectral bands instrument, and

the radiometry of pixels belonging to the same class corresponds to the average radiometry measured by this virtual instrument. Second, if a landscape object was not present in the ETM image due to a drastic landscape change, it will not be present in the merged image. In both cases, the landscape evolution is more likely to occur when time delay increases between ETM and MeRIS image acquisitions, and its effects on the fusion relevance can be evaluated by comparing the ERGAS values for different time delays.

## **7. CONCLUSION**

This paper shows how a MeRIS image can be merged with an ETM image in order to synthesize a new product with the best characteristics of each sensor, namely, the spatial resolution of ETM, and the spectral resolution and the frequent revisiting of MeRIS. The method, which had been tested on simulated MeRIS images before the launch of ENVISAT, was applied to real images over a coastal area. The effects of landscape evolution, which tend to increase as the time delay between the two acquisitions becomes longer, were analysed using the ERGAS parameter as a robustness criterion. The advantages and limitations of this resolution improvement method have been discussed. This experiment confirms the potential of this method for coastal water monitoring. However, a further validation should be carried out in areas where drastic changes are more frequent, like in tropical coastal zones.